

INTERVENING METAL SYSTEMS IN GRB AND QSO SIGHT LINES: THE Mg II AND C IV QUESTION¹

VLADIMIR SUDILOVSKY,^{2,3} SANDRA SAVAGLIO,³ PAUL VREESWIJK,⁴ CÉDRIC LEDOUX,⁴
 ALAIN SMETTE,⁴ AND JOCHEN GREINER³
Received 2007 May 5; accepted 2007 July 2

ABSTRACT

Prochter and coworkers recently found that the number density of strong intervening $0.5 < z < 2$ Mg II absorbers detected in gamma-ray burst (GRB) afterglow spectra is nearly 4 times larger than those in QSO spectra. We have conducted a similar study using C IV absorbers. Our C IV sample, consisting of a total of 19 systems, is drawn from three high-resolution and high to moderate signal-to-noise ratio VLT UVES spectra of three long-duration GRB afterglows, covering the redshift interval $1.6 < z < 3.1$. The column density distribution and number density of this sample do not show any statistical difference from the same quantities measured in QSO spectra. We discuss several possibilities for the discrepancy between C IV and Mg II absorbers and conclude that a higher dust extinction in the Mg II QSO samples studied up to now would give the most straightforward solution. However, this effect is only important for the strong Mg II absorbers. Regardless of the reasons for this discrepancy, this result confirms once more that GRBs can be used to detect a side of the universe that was unknown before, not necessarily connected with GRBs themselves, providing an alternative and fundamental investigative tool of the cosmic evolution of the universe.

Subject headings: cosmology: miscellaneous — gamma rays: bursts — quasars: absorption lines

Online material: color figures

1. INTRODUCTION

The advent of gamma-ray burst (GRB) exploration in the last 10 years has changed our view of the universe. These highly energetic events have been found over a very large interval of redshifts, from the local to $z = 6.3$ (Kawai et al. 2006). They are so bright that when one of these events occurs, the most remote structures can be temporarily “illuminated” and thus can be studied in unprecedented detail (Vreeswijk et al. 2005; Chen et al. 2005a). At $z > 1.5$, the optical (UV rest frame) afterglows of long-duration GRBs reveal properties of the forming universe never detected before, such as the existence of a population of metal-enriched, star-forming, and relatively small galaxies (Berger et al. 2006; D’Elia et al. 2007b; Fynbo et al. 2006; Prochaska et al. 2007; Savaglio 2006).

In a recent work, Prochter et al. (2006, hereafter P06) used GRBs to probe the galaxy halos distributed along GRB sight lines, similarly to what has been done for decades using quasars (QSOs). In their study, they identified 14 strong (equivalent width [EW] larger than 1 \AA) intervening Mg II absorbers in the sight lines of 14 long-duration GRBs. The total path length is $\Delta z = 15.5$ and the mean redshift is $\langle z \rangle = 1.1$, for a mean number density of $dn/dz = 0.90 \pm 0.24$. Surprisingly, only an incidence of 3.8 similar Mg II absorbers is expected for QSOs of the same path length. Dust extinction, gravitational lensing, different beam sizes, and systems belonging intrinsically to the GRB source were ruled out as possible explanations for this difference. Following such a result, Porciani et al. (2007) proposed that the different behavior of Mg II in GRB and QSO sight lines might be a combination of dust extinction bias, gravitational lensing, and absorbers being misidentified as intervening.

Particularly intriguing is the recent discovery of absorption variability in $z = 1.48$ Mg II and Fe II intervening systems along the GRB 060206 sight line over a time interval of a few hours (Hao et al. 2007). These authors support a scenario according to which the variability is expected if the size of the absorbing clouds is on the order of the GRB beam size (i.e., 10^{16} cm^{-2}), which expands faster than light (Loeb & Perna 1998) due to the large Lorentz factor. In addition, microlensing could also add to the possible cause of variability in this case, as described by Lewis & Ibata (2003).

In an effort to understand the reason for the Mg II discrepancy, we have considered intervening C IV absorbers in the lines of sight to GRB and QSO sources. It is important to note that the aforementioned effects act in a different way in C IV intervening systems for GRB and QSO sight lines. For instance, C IV is found at much larger impact parameters relative to Mg II, making gravitational lensing less effective. This also implies that the strength of Mg II absorption does not correlate to an increase in the strength of C IV absorption (York et al. 2006). Moreover, C IV absorbers do not trace dust to nearly the same extent as do Mg II absorbers. Effects from a partial covering factor of QSO background sources (due to a large QSO beam size; Frank et al. 2006) are ruled out for both C IV and Mg II absorbers, as this was never detected in high-resolution spectra with reasonable signal-to-noise ratios (S/Ns).

Both Mg II and C IV are easily detected due to their relatively high cosmic abundance, their large oscillator strength, and their appearance as doublets. C IV absorbers, a highly ionized species,⁵ are common features in the large Galactic halo (Chen et al. 2001), while strong Mg II absorbers are found at low impact parameters ($\rho \approx 15 \text{ kpc}$; Lanzetta & Bowen 1990). Strong Mg II systems with a rest equivalent width (W_r) in excess of 0.6 \AA are often associated with damped Ly α (DLA) systems (Rao et al. 2006; York et al. 2006). A direct comparison between the properties of C IV and Mg II absorbers is complicated by the fact that C IV can be effectively detected in the optical for $z > 1.8$, while Mg II is detected at lower redshifts ($0.2 < z < 2.3$).

¹ Based on observations collected at the European Southern Observatory, Chile; proposals 75.A-0385, 75.A-0603, and 77.D-0661.

² Physics Department, Guilford College, Greensboro, NC 27410.

³ Max-Planck-Institut für extraterrestrische Physik, Giessenbachstrasse, D-85748 Garching bei München, Germany.

⁴ European Southern Observatory, Alonso de Córdova 3107, Casilla 19001, Santiago 19, Chile.

⁵ The ionization potential of C IV is 64.5 eV, compared to 15.0 eV for Mg II.

TABLE 1
SAMPLE CHARACTERISTICS

SOURCE	z_{em}	z_{min}	z_{max}	NUMBER OF C IV SYSTEMS	FWHM (km s ⁻¹)	S/N ^a		
						$\lambda 1270$	$\lambda 1380$	$\lambda 1500$
GRB 050820	2.612	1.836	2.582	5	6.3	6	18	18
GRB 050922C	2.198	1.511	2.168	7	6.8	7	12	12
GRB 060607	3.082	2.205	3.052	7	6.9	58	...	61
Q1626+6433	2.320	1.607	2.290	15	6.6	88	128	137
Q1442+2931	2.661	1.875	2.631	14	6.6	113	107	121
Q1107+4847	2.966	2.114	2.936	11	6.6	90	94	81

^a S/N over 3 pixels outside the Ly α forest sampled near the three wavelengths $\lambda\lambda 1270$, 1380, and 1500 in the rest frame of the GRB or QSO.

Our C IV and Mg II survey in GRBs include optical spectra of five GRB afterglows taken with the high-resolution ($R > 42,000$) UV-optical echelle spectrograph UVES at the VLT (Vreeswijk et al. 2007). C IV absorbers in three sight lines are compared with those found in QSOs that cover very similar redshifts (Boksenberg et al. 2003). The cumulative number of absorbers as a function of redshift, as well as the column density distribution, are used to compare the incidence of C IV systems in sight lines of the GRBs and QSOs. Our Mg II sample is used to confirm the result obtained with equivalent widths.

In § 2, the data are presented. The methods for the analysis are presented in § 3, and the result and discussion are found in § 4. Throughout the paper we adopt a $h \equiv H_0/100 = 0.7$, $\Omega_m = 0.3$, and $\Omega_\Lambda = 0.7$ cosmology (Spergel et al. 2007).

2. THE DATA

GRB optical afterglow spectra of five GRBs were taken using the high-resolution spectrograph UVES. These are GRB 050730 at $z = 3.967$ (Chen et al. 2005b; D’Elia et al. 2007a), GRB 050820 at $z = 2.612$ (Ledoux et al. 2005; Prochaska et al. 2005), GRB 050922C at $z = 2.198$ (Jakobsson et al. 2005, 2006; Piranomonte et al. 2007), GRB 060418 at $z = 1.489$ (Dupree et al. 2006; Vreeswijk et al. 2007), and GRB 060607 at $z = 3.082$ (Ledoux et al. 2006). The spectra were normalized by fitting a polynomial function to the continuum. The spectra of GRB 050820, GRB 050922C, and GRB 060607 were used for the C IV sample, with a total absorption path length of $\Delta z = 2.25$ and a mean redshift of $\langle z \rangle = 2.63$. The two other GRB spectra, those of GRB 060418 and GRB 050730, were excluded from the sample, due to a lack of C IV redshift coverage and poor S/Ns. For the Mg II analysis, we used all these spectra, as the EWs are robust measurements when the S/N is not very high. The spectra used in the C IV survey all have a high S/N and high resolution (Table 1 and Fig. 1).

The QSO C IV sample (Boksenberg et al. 2003) has a very similar Δz and $\langle z \rangle$ of 2.26 and 2.65, respectively. A total of 20 C IV systems were identified in the GRB sample, and a total of 40 systems were identified in the QSO sample. The factor-of-2 difference in the number of systems is due to the higher S/N and thus lower detection limits of the QSO sample. Information specific to particular GRBs or QSOs can be found in Table 1.

The software package ESO-MIDAS and the program FITLYMAN were used to derive the column density, N , by simultaneously fitting Voigt profiles to both lines of the C IV doublet. If a system contained multiple components, the column density used was the sum of the column densities of the components.

2.1. C IV Selection Techniques

The C IV systems usually are well defined and have multiple absorption features with a velocity distribution structure of up to

a few hundred km s⁻¹ (Ellison et al. 2000; Boksenberg et al. 2003; Songaila 2005, 2006). One or more C IV “cloudlets” can compose a C IV system. Individual systems (i.e., belonging to one physical entity, such as a galaxy) are usually separated from each other by more than a few hundred km s⁻¹ and are often associated with Ly α absorption. In two cases, several C IV absorption features that share the same Ly α absorption were classified as two distinct systems. All other C IV absorption features associated with distinct Ly α absorption are considered to be individual systems. The velocity spread of these C IV absorption features would have been in excess of 600 km s⁻¹ if they had been classified as one system. The column density of the C IV system is the sum of the column densities of all of its constituent cloudlets. Velocity profiles of all identified systems are found in Figure 1. Table 2 presents the redshift, column density $N_{\text{C IV}}$, and Doppler parameter b of all of the C IV systems detected in the GRB sample.

In this study, only C IV systems outside of the Ly α forest (i.e., $z \geq [1215.67(1 + z_{\text{em}})/1548.1949] - 1$) are included in the sample. No systems within $\Delta v = 2300$ km s⁻¹ (corresponding to a physical separation of 5.5 Mpc at $z = 2.3$) of the redshift of the GRB or QSO were included, so as to prevent any unknown differential effects between the GRB and QSO host environment. A total of three C IV systems were excluded from the QSO sample, as well as one system from the GRB sample.

2.2. Completeness Limit

Since the S/Ns in the spectra vary, we derived the lowest detection limit in our GRB sample. A completeness limit of 1 Å rest equivalent width ($W_r \geq 1$ Å) was used by P06 for the Mg II sample. In this study, column density is used as the parameter to determine completeness. A theoretical rest equivalent width limit of 3σ is derived from the various error spectra for the weaker line of the doublet (C IV $\lambda 1550$). Since the ratio of the stronger to the weaker line is 2:1, for small absorptions (i.e., in the linear part of the curve of growth), this corresponds to a detection limit of 6σ for the stronger line (C IV $\lambda 1548$). When combined with the fact that C IV systems are identified by the presence of *both* of these lines, our C IV detection limit is conservative and is $>6\sigma$.

This value is converted to a column density limit for a given Doppler parameter b from the linear portion of the empirical curve of growth of C IV. The final column density limit for the survey is the maximum column density limit among the six spectra of the three GRBs (Fig. 2). Limits were calculated using $b = [5, 10, 15]$ km s⁻¹ (Fig. 2, *colored lines, from bottom to top*). We note that the mean Doppler parameter in the sample is $\langle b \rangle = 14.5$ km s⁻¹ and that large b -values are typically associated with large values of the C IV column density, which are easy to detect.

As our S/N does not vary much for $z < 2.3$ and for $z > 2.3$ (apart from two small redshift bins), we have chosen for the final

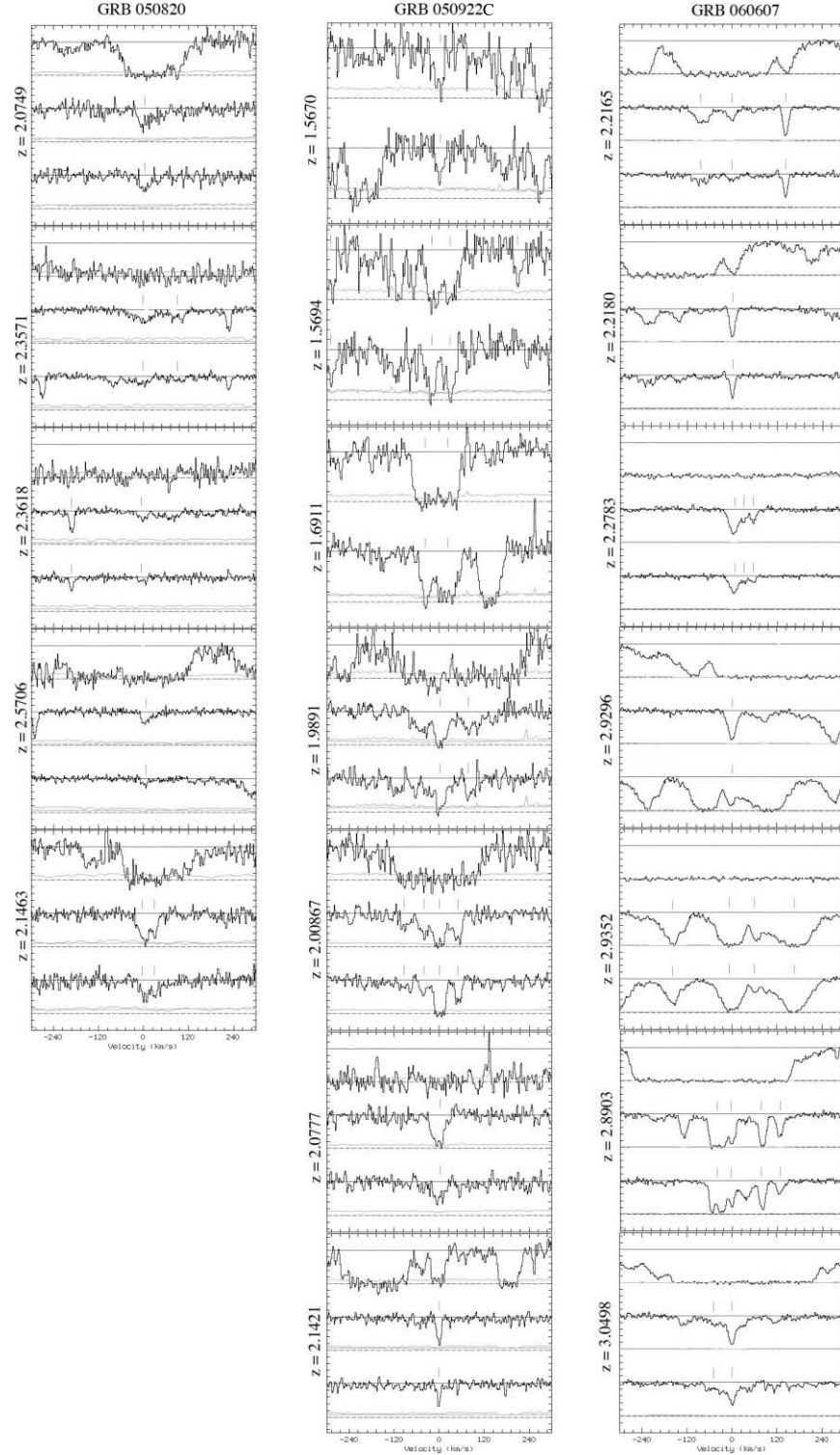


FIG. 1.— Normalized flux vs. velocity profiles for C IV systems in the three GRBs studied. From left to right are the profiles for GRB 050820, GRB 050922C, and GRB 060607, respectively. The gray lines represent the associated error spectra. The subpanels, from top to bottom, plot Ly α (when applicable), C IV λ 1548, and C IV λ 1550. [See the electronic edition of the *Journal* for a color version of this figure.]

analysis a conservative limit close to the $b = 15 \text{ km s}^{-1}$ line, described by a step function, with $N_{\text{lim}} = 10^{13} \text{ cm}^{-2}$ and $N_{\text{lim}} = 10^{12.7} \text{ cm}^{-2}$ in the lower and higher redshift bins, respectively (Fig. 2, *dashed line*). As the average resolutions of the GRB and QSO spectra are within 5% of each other and are all well above the value with which to resolve the C IV doublet, it is not necessary to compensate for different resolutions when comparing the dif-

ferent spectra (Table 1). The black and gray points in Figure 2 represent the measured GRB C IV and QSO C IV column densities, respectively.

2.3. The QSO Sample

Our QSO sample comes from a larger sample of quasars used by Boksenberg et al. (2003). We use their identification of C IV

TABLE 2
C IV SYSTEMS

System	z_{abs}	$\log N_{\text{C IV}}$ (cm^{-2})	b (km s^{-1})
GRB 050820			
1.....	2.0749	13.64	22.1
2.....	2.1463	13.43	23.3
		13.33	6.1
3.....	2.3571	13.43	23.3
		12.83	6.5
		13.21	5.9
4.....	2.3618	13.05	17.4
5.....	2.5706	13.12	14.5
GRB 050922C			
1.....	1.5670	13.78	14.7
2.....	1.5694	14.20	14.1
		14.20	18.2
3.....	1.6911	14.44	25.3
		14.61	20.9
4.....	1.9891	14.26	13.1
		13.55	12.7
5.....	2.0087	13.60	15.7
		17.20 ^a	5.6
		13.73	11.3
6.....	2.0778	13.89	17.9
7.....	2.1421	13.47	5.1
GRB 060607			
1.....	2.2165	13.59	28.4
		13.21	15.5
2.....	2.2180	13.55	6.6
3.....	2.2783	13.64	13.8
		12.95	8.2
		13.01	8.6
4.....	2.8903	14.12	5.6
		14.27	11.7
		13.75	7.8
		13.95	8.0
		13.42	9.8
5.....	2.9296	13.71	12.0
6.....	2.9352	14.14	27.4
		14.54	28.8
		14.68	35.7
7.....	3.0498	13.19	20.2
		13.70	11.1

^a Heavily saturated.

systems and column densities, and we derived cumulative numbers and column density distribution from their tables. The resolution and redshift range of the QSO sample are very similar to those of the GRB sample. However, the S/N is significantly higher in the QSO sample (Table 1).

3. METHODS

3.1. Mg II Absorbers in the GRB Sight Lines

To verify that the overdensity of Mg II systems along GRB sight lines is not due to the inhomogeneity of the P06 sample, we have performed the same analysis on our homogeneous sample of UVES spectra using exactly the same search criteria. We note that two UVES afterglow sight lines are not in the P06 sample: GRB 050922C and GRB 060607. Table 3 shows the GRB sight lines used, the starting and ending redshift of the potential Mg II

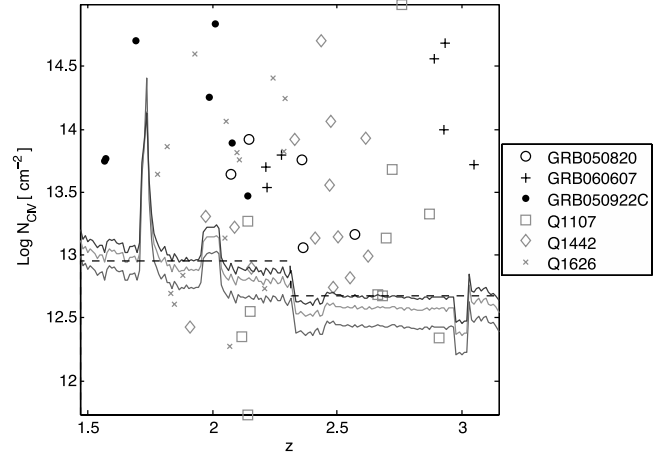


FIG. 2.— Column density of C IV systems, measured in GRB (black symbols) and QSO (gray symbols) sight lines, respectively, as a function of redshift. The lines represent the completeness limit to detect lines at a $>6\sigma$ confidence level. From bottom to top, the limits for $b = [5, 10, 15] \text{ km s}^{-1}$ are plotted. The dashed line represents the limit used in this study. [See the electronic edition of the Journal for a color version of this figure.]

system, the redshifts of the identified Mg II systems, and the rest-frame equivalent width that we measured.

The total redshift path covered by the UVES sample is $dz = 6.75$, with a mean redshift of $\langle z \rangle = 1.3$. We find six Mg II systems with a rest-frame equivalent width larger than unity. This corresponds to a number density of $dn/dz = 0.89 \pm 0.36$, consistent with the value of $dn/dz = 0.90 \pm 0.24$ found by P06, at a mean redshift of $\langle z \rangle = 1.1$.

Although our redshift path is smaller than that of P06, our sample of UVES spectra is homogeneous and of much higher quality, and it provides a preliminary confirmation of the Mg II excess observed in GRB sight lines. As the sample grows, a more sophisticated analysis will be possible, such as the one we present in the following sections on the C IV systems.

3.2. Cumulative Number of C IV Systems versus z

The cumulative number of C IV systems as a function of redshift is shown in Figure 3 for the QSO and GRB samples. A bin size of $\Delta z = 0.25$ was used, and error bars were calculated assuming a Poisson distribution, where $\sigma \propto \sqrt{n}$, with n being the number of C IV systems. In addition to providing an easy visual comparison with the results obtained by P06, this method has the

TABLE 3
IDENTIFIED Mg II SYSTEMS IN THE UVES SAMPLE

GRB	z_{GRB}	z_{start}	z_{end}	z_{abs}	$W_r(2796 \text{ \AA})^a$
050730.....	3.9686	1.160	2.0	1.7734	0.913 ± 0.008
050820.....	2.6145	0.572	2.0	0.6915	2.896 ± 0.017
				1.4288	1.329 ± 0.022
				1.6204	0.238 ± 0.009
050922C.....	2.1991	0.391	2.0	0.6369	0.167 ± 0.009
				1.1068	0.589 ± 0.024
060418.....	1.4900	0.359	2.0	0.6026	1.257 ± 0.008
				0.6558	1.071 ± 0.008
				1.1069	1.836 ± 0.006
060607.....	3.0748	0.772	2.0	1.5103	0.199 ± 0.006
				1.8033	1.906 ± 0.008

^a The error on the equivalent width is calculated from the noise spectrum; an error on the continuum normalization has not been included.

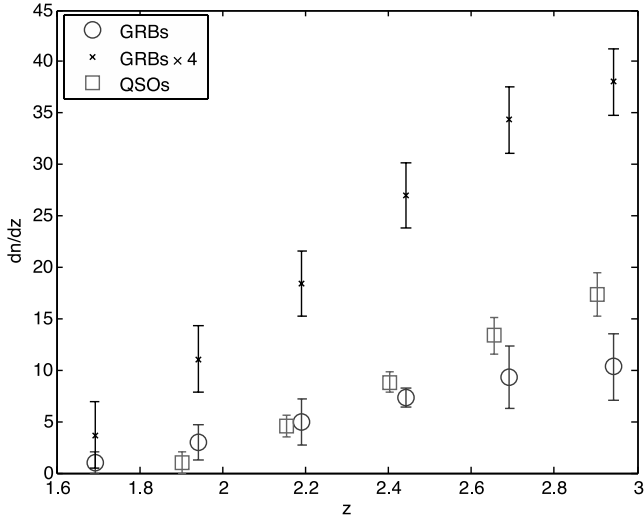


FIG. 3.—Cumulative number of C IV systems in GRB (circles) and QSO (squares) sight lines, per redshift bin of $\Delta z = 0.25$, as a function of redshift. The data designated as “GRBs $\times 4$ ” (crosses) represent an incidence of 4 times as many C IV systems as were actually measured. [See the electronic edition of the Journal for a color version of this figure.]

potential to amplify systematic differences in the number of C IV systems that are too small to see on a redshift bin-by-bin basis.

Figure 3 shows no significant difference between the GRB and QSO samples. The detection limit discussed in § 2.2 was applied to both the GRB and QSO subsamples. To demonstrate that an excess of ~ 4 times as many Mg II systems as were actually observed would be easily detected in our C IV study, we multiply by 4 the cumulative number of C IV systems measured in the GRB sample (Fig. 3, crosses).

In addition, the data were split into two subsamples on the basis of column densities: $N_{\text{C IV}} > 10^{13.8} \text{ cm}^{-2}$ and $N_{\text{C IV}} \leq 10^{13.8} \text{ cm}^{-2}$. This corresponds to the median column density of the full C IV sample. Although in § 1 we mentioned that there has not been a relationship established between C IV and Mg II systems, we split the sample to test if there was any difference in C IV systems based on their absorption strength. Again, there is no detectable difference in the number density of C IV systems for GRB or QSO sight lines, although small-number statistics play a more significant role for the subsamples than in the full sample.

3.3. Column Density Distribution

The number of C IV systems per column density interval and absorption path length, $d^2n/dN dX$, in GRBs is compared with the same function derived from QSOs. The absorption path length is defined as

$$dX = \frac{1+z}{\sqrt{\Omega_m(1+z) + \Omega_\Lambda/(1+z)^2}} dz. \quad (1)$$

We selected a column density interval of $dN = 10^{0.3} \text{ cm}^{-2}$, while $z \equiv \langle z \rangle = 2.37$ corresponds to the mean redshift of the sample. The redshift bin dz is the total redshift interval covered by all sources, from z_{min} to z_{max} , as described in § 2.1.

Using the column density distribution to compare the incidence of C IV systems allows one to account for multiple redshift coverage, as well as to compare systems in spectra with different S/Ns, without discarding any data due to different completeness limits. In addition, the column density distribution provides an

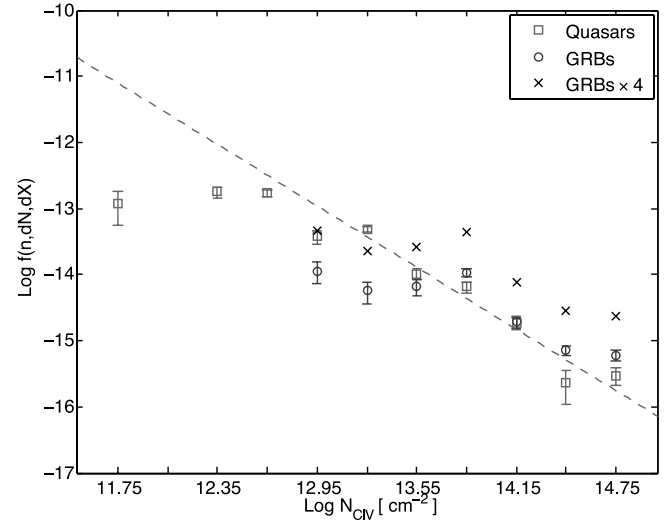


FIG. 4.—Column density distribution of the GRB (circles) and QSO (squares) samples. Plotted with black crosses is the column density distribution of 4 times as many C IV systems as there actually were. The data are best fitted by a line with a slope of -1.5 ± 0.2 (-1.2 ± 0.5) and an offset of 6 ± 3 (3 ± 6) for the QSO (GRB) sample. The best fit for the QSO sample is plotted as a dashed line. [See the electronic edition of the Journal for a color version of this figure.]

easy comparison of the incidence of strong and weak absorbers alike in different lines of sight.

In Figure 4 we show the results. The sample completeness is demonstrated by the flattening of the power-law distribution, which happens at $\log N_{\text{C IV}} = 13.6$ and $\log N_{\text{C IV}} = 12.6$ for the GRB and QSO samples, respectively. The two column density distributions above these limits are best fitted with a power law of the form $dn/dN \propto N^{-\beta}$, where $\beta = 1.5 \pm 0.2$ for the QSOs and $\beta = 1.2 \pm 0.5$ for the GRBs.

As in the case of the cumulative number of C IV systems, the C IV column density distributions in the GRB and QSO sight lines are consistent. We also show that an excess of 4 times as many systems would show a clear deviation of the two distributions.

4. RESULTS

We have studied the statistical difference between intervening absorbers in GRB and QSO sight lines. Our Mg II sample confirms the overdensity detected by P06 in GRB sight lines. On the other hand, there is no statistical difference in the number of C IV systems, considering both the cumulative number and the column density distribution. Mg II and C IV do not behave in the same way. We consider the effects of dust extinction, gravitational lensing, and absorbers associated with the circumburst environment in the following subsections. We note that the redshift intervals covered by the C IV and Mg II absorbers are different, with $1.6 < z < 3.1$ for the former and $0.5 < z < 2$ for the latter.

4.1. Dust Extinction

It has been suggested that QSO surveys are biased against strong absorbers distributed along the sight lines because dust can obscure the background source (Fall & Pei 1993; Smette et al. 2005). The dust extinction in C IV absorbers is negligible. To estimate this, we consider that the typical column density in the observed GRB and QSO samples of intervening C IV systems is $N_{\text{C IV}} < 10^{14.8} \text{ cm}^{-2}$. It is reasonable to believe that the carbon is marginally depleted in dust grains (Savage & Sembach 1996). We assume that most of the carbon in these gas clouds is in C IV form and that the dust-to-metals ratio is as in the Large Magellanic Cloud (LMC; Bohlin et al. 1978). Following Savaglio & Fall

(2004), we estimate dust extinction by making the basic assumption that it is proportional to the total column density of metals. A correction that must be applied in the case of a refractory and/or ionized heavy element species is considered. However, no correction is necessary if the heavy element considered is not depleted in dust and the ionization correction is negligible. Using the LMC dust-to-metals ratio and the C IV column density yields an upper limit to the visual and UV dust extinctions of $A_{1500} = 0.003$ and $A_V = 0.001$, respectively, for $N_{C\,IV} < 10^{14.8} \text{ cm}^{-2}$. One should recall that the LMC dust-to-metals ratio is generally small compared to other regions of the dense ISM in the Milky Way and that C IV is a high-ionization species and thus a large ionization correction is necessary to get the total carbon column density. If carbon is only present 10% of the time in C IV form and the dust-to-metals ratio is 10 times higher than that in the LMC (perhaps as in the Galactic cool ISM), the extinction would be 100 times larger, but still negligible, even in the UV.

The picture could be different for the Mg II absorbers selected by P06. The dust depletion of magnesium in the Galaxy is anywhere between 70% and 95%, from the warm diffuse to the cool diffuse ISM (Savage & Sembach 1996). The selection by P06 of $W_r(2796 \text{ \AA}) > 1 \text{ \AA}$ corresponds to an approximate Mg II column density limit of $N_{Mg\,II} \approx 10^{14} \text{ cm}^{-2}$. For $N_{Mg\,II} = 10^{14} \text{ cm}^{-2}$, the dust extinction is reasonably negligible, assuming a LMC extinction law. However, the dust extinction grows linearly with the metal column density if the dust-to-metals ratio is constant (Savaglio & Fall 2004). For $W_r(2796 \text{ \AA}) > 1.5 \text{ \AA}$ (half of the Mg II absorbers in the P06 sample and the present UVES sample) we derive $N_{Mg\,II} \approx 10^{15} \text{ cm}^{-2}$, and thus $A_{1500} > 0.07$ and 0.7 in the cases of warm diffuse and cool diffuse ISM, respectively.

Although dust cannot explain the difference for the $W_r = 1 - 1.5 \text{ \AA}$ absorbers, the detection can be more complicated for stronger absorbers with $W_r > 1.5 \text{ \AA}$, which is more than half of the P06 sample. This is particularly true if these absorbers are characterized by a dust depletion as in the Galactic cool ISM.

There has been extensive debate on the topic of dust extinction in QSOs. Ellison et al. (2004) found no significant selection biases associated with the Sloan Digital Sky Survey (SDSS) QSO data in the CORALS survey. However, the sample at $0.6 < z < 1.7$ includes all Mg II absorbers with $W_r > 0.3 \text{ \AA}$, which mostly do not affect the background source. Indeed, Nestor et al. (2006) found that the column density distribution of weak Mg II absorbers is different than that for strong absorbers, which could suggest an evolving dust extinction bias with column density. York et al. (2006) found a negligible extinction of $E_{B-V} < 0.001$ for sight lines of Mg II systems with $W_r < 1.5 \text{ \AA}$, in agreement with our expectations. The extinction is slightly higher above this limit. Vladilo & Péroux (2005) find that dust extinction becomes significant ($A_V \approx 0.15 \text{ mag}$) as the column density of Zn II approaches $10^{12.8} \text{ cm}^{-2}$, which in turn corresponds to a Mg II value of $W_r \approx 3 \text{ \AA}$ (Turnshek et al. 2005; Vladilo 2005). Although 3 \AA is an unusually strong absorption, it is unclear at what Mg II EW between $W_r \approx 1.5 \text{ \AA}$ and $W_r \approx 3 \text{ \AA}$ dust extinction does start to affect surveys. Interestingly, Wild & Hewett (2005) and Wild et al. (2006) found that strong Ca II absorbers at $0.8 < z < 1.3$ are missed by the SDSS due to dust obscuration. The EW of Mg II associated with these Ca II absorbers is typically above 2 \AA .

It is intriguing that Ellison et al. (2006) found evidence of large dust depletion in intervening Mg II absorbers along GRB 060418. For one of the absorbers, at $z = 1.11$, a 2200 \AA bump, typical in the Galactic extinction, was clearly detected for the first time at high redshift. This has yet to be found in QSO spectra.

Although most surveys suggest that there is no selection bias associated with dust extinction in QSO spectra, this statement is

valid for the total population of QSO absorbers, which are dominated by weak absorbers. Furthermore, these do not affect the background light. Although the purpose of this survey is not to quantify the amount of dust extinction in QSO or GRB lines of sight, the results obtained by both P06 and us do not exclude these arguments.

4.2. Gravitational Lensing

A similar selection bias can occur when the background source is magnified through gravitational lensing. The amount of magnification depends on the source beam size with respect to the Einstein radius of the lens, where the amplification is larger for a smaller source beam size (Chang & Refsdal 1979). If it is indeed the case that GRB beams are smaller than QSO beams, gravitational magnification could be stronger for GRBs than for QSOs.

However, a larger amplification of GRBs is not enough (see, e.g., Smette et al. 1997). The optical depth for lensing (macro- or microlensing) is maximal if the redshift of the lens is $z_l \sim 0.7$ (it decreases to half the maximum roughly within $\Delta z = \pm 0.3$) for background sources (GRBs or QSOs) at $z_s \gg 1$. For background sources at $z_s \sim 1$ or less, the optical depth is maximal at $z_l \sim z_s/2$. Therefore, if lensing is really at play, then most Mg II absorbers would follow this. This is not the case for the Mg II absorbers. About 60% (10 out of 16) of the GRBs studied by P06 and us are at $z_s > 2$, and of these, the foreground Mg II absorbers are mostly at $z_l > 1$. For the remaining 40% of the GRB sample, all but one have $z_s > 1$ and $z_l > z_s/2$.

Porciani et al. (2007) tentatively found that afterglows with more than one Mg II absorber are on average 1.7 times brighter than their counterparts. This is based on the optical luminosity measured 12 hr after the burst (Nardini et al. 2006). We performed a similar check using the *B*-band absolute magnitudes calculated 1 day after the burst by Kann et al. (2006) and D. A. Kann & S. Klose (2007, in preparation). These are available for 8 of the 14 GRB sight lines in the P06 Mg II sample. More appropriately, we considered the number density (the number of Mg II absorbers per unit redshift) for each sight line, instead of the total number of Mg II absorbers. We do not detect any correlation between the brightness of the GRB and the number density of the Mg II absorbers. This test does not confirm the magnification hypothesis, although it cannot exclude it on its own.

Porciani et al. (2007) suggest that up to 30% of *Swift* GRBs could be microlensed, making optical spectra easier to take. Microlensing could also give rise to time variability, following a scenario similar to the one considered by Lewis & Ibata (2003), which would explain this effect found for Fe II and Mg II absorbers by Hao et al. (2007). Although a survey of C IV would be less affected by macrolensing due to foreground galaxies than would a survey of Mg II, this is not the case for microlensing (microlenses are randomly distributed, whereas macrolensing becomes increasingly significant with decreasing impact parameters). For this reason, it is unclear what significance these results have for the hypothesis that gravitational lensing plays a role in the number density of C IV.

4.3. Absorbers Associated with the GRB Host Environment

It is generally accepted that metals that are ejected at semi-relativistic speeds from QSO or GRB sources would have distinctively broad profiles. These features can be found in QSOs up to $\Delta v \approx 50,000 \text{ km s}^{-1}$ away from the source and are known as broad absorption lines (BALs; Hamann et al. 1993). However, there has been no evidence that suggests that the same process occurs in GRBs. In fact, BALs are mostly detected in high-ionization absorption lines, which are naturally expected for gas clouds very close to a very luminous source. Therefore, if it is

detected for Mg II absorbers, it should be even stronger for C IV. Moreover, as relativistic speeds are expected, the absorption features should be very large in the velocity space. This is clearly seen in BALs, but is not at all present in normal intervening Mg II or C IV absorbers.

The scenario proposed by Porciani et al. (2007), in which a supernova remnant with multiple high-velocity Mg II “clouds” that is associated with the GRB and its environment would give a Mg II number excess, is not supported by our results. It is true that this effect might be less significant in C IV absorbers because the intrinsic number density of intervening systems is large and the contamination can only be small. Since there are generally few Mg II absorption systems per sight line, this misidentification can significantly affect statistics. This scenario must only occur once or twice among the 14 GRBs in the Mg II sample to significantly affect results. However, such high-velocity absorbers would require velocities of the gas of half the speed of light to be misidentified as an “intervening absorber.” This is not typically observed in supernova remnants. Intrinsic broadening of the absorbing features is also expected to be much larger than that observed.

5. SUMMARY

An excess of Mg II intervening absorbers along high- z GRB sight lines relative to similar absorbers found in high- z QSO spectra was recently found. These Mg II absorbers trace galaxies that intersect bright background point sources. The total number of absorbers in GRB sight lines is nearly 4 times higher in the interval $0.5 < z < 2$ (Prochter et al. 2006).

We have performed a similar study using an additional sample of Mg II absorbers and confirm the previous results. We additionally investigate intervening C IV absorbers and adopt a more detailed analysis. We have compared the number density and column density distribution in three GRB sight lines in the range $1.6 < z < 3.1$ with the same quantities in QSO sight lines in a similar redshift interval. There is no detectable difference in the incidence of C IV systems in the two samples, contrary to that found for Mg II.

Observationally, the main differences between the C IV and Mg II absorbers are the larger impact parameter, the smaller dust extinction, the higher ionization level, the higher redshift, and the larger number density dn/dz of the former with respect to the latter. We expect one or more of these factors to be directly or indirectly responsible for the discrepancy.

We exclude the possibilities that some of the intervening Mg II or C IV absorbers could be intrinsically associated with the GRBs, or that these absorbers could have a partial covering factor in QSO spectra. We have shown that the scenario in which statistics being affected through the misidentification of intrinsic

systems as intervening systems is unlikely, especially in a survey of C IV absorbers.

Out of the possible effects, dust extinction could cause part of the difference in Mg II absorbers. This is due to the fact that QSO studies are generally performed on the bright population, whereas GRBs are primarily selected because of their gamma-ray signal. However, we have shown that dust gives a sizable effect only for the strong Mg II absorbers, those with $W_r > 1.5 \text{ \AA}$, which is half of the total sample used by P06. This is true for normal dust, however, that has a dust-to-metals ratio similar to that of the Milky Way. If the dust-to-metals ratio is larger than what was previously thought for at least a fraction of high- z galaxies, the effects of dust extinction would become more pronounced.

In the future, better statistics for both C IV and Mg II absorbers in GRB spectra will help to solve the issue. Fe II absorbers could be used to probe the same galaxy regions as Mg II absorbers. The advantages of using Fe II are its larger redshift range (for a higher number statistics) and its less complicated access to column density. The column density is a more meaningful parameter than the equivalent width, which we used for Mg II. A further test would be to study the mean Ly α absorption in the diffuse IGM, which is well studied from QSO spectra and relatively easy to measure in GRB spectra, provided that statistical methods are used, such as the IGM optical method (Fan et al. 2006).

GRB afterglow studies have already demonstrated that there is a population of absorbers identified as GRB DLAs and intrinsic to the GRB host that were very hard to detect before and that show on average very strong absorption features (Savaglio et al. 2003; Berger et al. 2006; Fynbo et al. 2006). It is not known whether the existence of this population is intrinsic to the GRB itself or common in the high- z universe. The study of intervening absorbers presented in this work may show that GRBs are probing the high- z universe better than QSO studies, regardless of the nature of the GRB itself. The results of our work are not conclusive, but they do imply that there may be fundamental assumptions about the structure of the universe and our methods to probe it that need to be reconsidered.

The authors thank Alec Boksenberg, Alex Kann, Cristiano Porciani, and Tony Songaila for interesting comments. The authors especially thank Sara Ellison for sharing her insights concerning dust extinction and offering suggestions for follow-up work. V. S. acknowledges the generosity of the Winslow Womack grant awarded by Guilford College for undergraduate research and the kind hospitality of the Max Planck Institute for Extraterrestrial Physics, at which a large part of this work was performed.

REFERENCES

- Berger, E., Penprase, B. E., Cenko, S. B., Kulkarni, S. R., Fox, D. B., Steidel, C. C., & Reddy, N. A. 2006, *ApJ*, 642, 979
 Bohlin, R. C., Savage, B. D., & Drake, J. F. 1978, *ApJ*, 224, 132
 Boksenberg, A., Sargent, W. L. W., & Rauch, M. 2003, *ApJS*, submitted (astro-ph/0307557)
 Chang, K., & Refsdal, S. 1979, *Nature*, 282, 561
 Chen, H.-W., Lanzetta, K. M., Webb, J. K., & Barcons, X. 2001, *ApJ*, 559, 654
 Chen, H.-W., Prochaska, J. X., Bloom, J. S., & Thompson, I. B. 2005a, *ApJ*, 634, L25
 Chen, H.-W., Thompson, I., Prochaska, J. X., & Bloom, J. 2005b, *GCN Circ.* 3709, <http://gc.gsfc.nasa.gov/gcn/gcn3/3709.gcn3>
 D’Elia, V., Piranomonte, S., Ward, P., Fiore, F., Meurs, E. J. A., Norci, L., & Vergani, S. D. 2007a, in *AIP Conf. Ser.* 924, *The Multicolored Landscape of Compact Objects and Their Explosive Origins*, ed. T. Di Salvo et al. (New York: AIP), 429
 D’Elia, V., et al. 2007b, *A&A*, 467, 629
 Dupree, A. K., Falco, E., Prochaska, J. X., Chen, H.-W., & Bloom, J. S. 2006, *GCN Circ.* 4969, <http://gc.gsfc.nasa.gov/gcn/gcn3/4969.gcn3>
 Ellison, S. L., Churchill, C. W., Rix, S. A., & Pettini, M. 2004, *ApJ*, 615, 118
 Ellison, S. L., Songaila, A., Schaye, J., & Pettini, M. 2000, *AJ*, 120, 1175
 Ellison, S. L., et al. 2006, *MNRAS*, 372, L38
 Fall, S. M., & Pei, Y. C. 1993, *ApJ*, 402, 479
 Fan, X., et al. 2006, *AJ*, 132, 117
 Frank, S., Bentz, M. C., Stanek, K. Z., Dietrich, M., Mathur, S., Peterson, B. M., & Atlee, D. W. 2006, *ApJ*, submitted (astro-ph/0605676)
 Fynbo, J. P. U., et al. 2006, *A&A*, 451, L47
 Hamann, F., Korista, K. T., & Morris, S. L. 1993, *ApJ*, 415, 541
 Hao, H., et al. 2007, *ApJ*, 659, L99
 Jakobsson, P., Fynbo, J. P. U., Paraficz, D., Telting, J., Jensen, B. L., Hjorth, J., & Castro Cerón, J. M. 2005, *GCN Circ.* 4017, <http://gc.gsfc.nasa.gov/gcn/gcn3/4017.gcn3>
 Jakobsson, P., et al. 2006, *A&A*, 460, L13
 Kann, D. A., Klose, S., & Zeh, A. 2006, *ApJ*, 641, 993
 Kawai, N., et al. 2006, *Nature*, 440, 184
 Lanzetta, K. M., & Bowen, D. 1990, *ApJ*, 357, 321

- Ledoux, C., Vreeswijk, P., Smette, A., Jaunsen, A., & Kaufer, A. 2006, GCN Circ. 5237, <http://gcn.gsfc.nasa.gov/gcn/gcn3/5237.gcn3>
- Ledoux, C., et al. 2005, GCN Circ. 3860, <http://gcn.gsfc.nasa.gov/gcn/gcn3/3860.gcn3>
- Lewis, G. F., & Ibata, R. A. 2003, MNRAS, 340, 562
- Loeb, A., & Perna, R. 1998, ApJ, 495, 597
- Nardini, M., Ghisellini, G., Ghirlanda, G., Tavecchio, F., Firmani, C., & Lazzati, D. 2006, A&A, 451, 821
- Nestor, D. B., Turnshek, D. A., & Rao, S. M. 2006, ApJ, 643, 75
- Piranomonte, S., D'Elia, V., Ward, P., Fiore, F., & Meurs, E. J. A. 2007, Nuovo Cimento, in press (astro-ph/0701563)
- Porciani, C., Viel, M., & Lilly, S. J. 2007, ApJ, 659, 218
- Prochaska, J. X., Bloom, J. S., Wright, J. T., Butler, R. P., Chen, H. W., Vogt, S. S., & Marcy, G. W. 2005, GCN Circ. 3833, <http://gcn.gsfc.nasa.gov/gcn/gcn3/3833.gcn3>
- Prochaska, J. X., et al. 2007, ApJS, 168, 231
- Prochter, G. E., et al. 2006, ApJ, 648, L93 (P06)
- Rao, S. M., Turnshek, D. A., & Nestor, D. B. 2006, ApJ, 636, 610
- Savage, B. D., & Sembach, K. R. 1996, ARA&A, 34, 279
- Savaglio, S. 2006, New J. Phys., 8, 195
- Savaglio, S., & Fall, S. M. 2004, ApJ, 614, 293
- Savaglio, S., Fall, S. M., & Fiore, F. 2003, ApJ, 585, 638
- Smette, A., Claeskens, J.-F., & Surdej, J. 1997, NewA, 2, 53
- Smette, A., Wisotzki, L., Ledoux, C., Garcet, O., Lopez, S., & Reimers, D. 2005, in IAU Colloq. 199, Probing Galaxies through Quasar Absorption Lines, ed. P. R. Williams, C.-G. Shu, & B. Menard (Cambridge: Cambridge Univ. Press), 475
- Songaila, A. 2005, AJ, 130, 1996
- . 2006, AJ, 131, 24
- Spergel, D. N., et al. 2007, ApJS, 170, 377
- Turnshek, D. A., Rao, S. M., Nestor, D. B., Belfort-Mihalyi, M., & Quider, A. M. 2005, in IAU Colloq. 199, Probing Galaxies through Quasar Absorption Lines, ed. P. R. Williams, C.-G. Shu, & B. Menard (Cambridge: Cambridge Univ. Press), 104
- Vladilo, G. 2005, in IAU Colloq. 199, Probing Galaxies through Quasar Absorption Lines, ed. P. R. Williams, C.-G. Shu, & B. Menard (Cambridge: Cambridge Univ. Press), 325
- Vladilo, G., & Péroux, C. 2005, A&A, 444, 461
- Vreeswijk, P., Ellison, S., Ledoux, C., Wijers, R., & Hjorth, J. 2005, in ASP Conf. Ser. 344, The Cool Universe: Observing Cosmic Dawn, ed. C. Lidman & D. Alloin (San Francisco: ASP), 79
- Vreeswijk, P. M., et al. 2007, A&A, 468, 83
- Wild, V., & Hewett, P. C. 2005, MNRAS, 361, L30
- Wild, V., Hewett, P. C., & Pettini, M. 2006, MNRAS, 367, 211
- York, D. G., et al. 2006, MNRAS, 367, 945